Engineering Science
2026, Vol. 11, No. 3, pp. 69–74
https://doi.org/10.11648/j.es.20261103.12

Research Article

Predictive-Experimental Modeling of Biocementation (MICP) for the Reliability-Based Design of Shallow Foundations in Lima Silty Sands

Cleto Mauricio Vidal Lopez*

Department of Geotechnical Engineering, Faculty of Civil Engineering, Universidad Nacional Federico Villarreal, Lima, Peru

Abstract

Context: Urban expansion in Lima has forced the occupation of low-compaction aeolian deposits in high-vulnerability sectors like Lomo de Corvina and Villa El Salvador. Objective: This study develops and validates a predictive-experimental microbially induced calcite precipitation (MICP) model based on reliability engineering to quantify and reduce geotechnical uncertainty in shallow foundations. Methodology: Cylindrical specimens of aeolian sand were extracted and inoculated with *Sporosarcina pasteurii* (OD600: 0.8-1.2) and subjected to equimolar cementation cycles of urea and $CaCl_2$ (0.5 M) every 12 hours. Geomechanical performance was evaluated through direct shear and load tests, and the mechanical variability was rigorously quantified via Monte Carlo simulations operating over 10,000 iterations to compute limit state functions under local building standards. Results: Biocementation promoted a fundamental transition toward a highly predictable geomechanical system (R^2 =0985 for the biogenic cohesion-friction correlation and R^2 = 0.992 for settlement control). The internal friction angle increased from 31.0 °to 34.5 °while inducing effective biogenic cohesion, resulting in a 304% increase in allowable bearing capacity (q_{adm}), reaching up to 4.85 kg/cm^2. Serviceability Limit State (SLS) design settlements stabilized tightly at 1.45 cm. Conclusions: The biochemical treatment elevates the structural reliability index (β) from a critical baseline of 2.1 to a high-safety target of 3.5. This mathematical enhancement drastically reduces operational failure probability below 0.01%, successfully complying with the stringent requirements of the E.030 and E.050 Peruvian Technical Standards.

Keywords

Microbially Induced Calcite Precipitation (MICP), Reliability Engineering, Allowable Bearing Capacity, Eolian Sand, Monte Carlo Simulation, Serviceability Limit State

1. Introduction

The coastal geology of Lima, particularly in the expansion zones of Lomo de Corvina and Villa El Salvador, is characterized by extensive aeolian sand deposits. Geotechnically, these soils present low relative density, poor gradation, and lack of cohesion, positioning them as highly vulnerable areas under seismic conditions [1, 2]. Traditional stabilization techniques often involve high carbon footprints or alter local hydrogeology [3, 4].

*Correspondence: Cleto Mauricio Vidal Lopez (cvidal@unfv.edu.pe)

Received: 16 July 2026; **Accepted:** 28 July 2026; **Published:** 16 November 2026

Copyright: © The Author(s), 2026. Published by Science Publishing Group. This is an **Open Access** article, distributed under the terms of the Creative Commons Attribution 4.0 License (http://creativecommons.org/licenses/by/4.0/), which permits unrestricted use, distribution and reproduction in any medium, provided the original work is properly cited.

In this context, Microbially Induced Calcite Precipitation (MICP) emerges as a sustainable and synergetic biochemical alternative [5, 6]. Utilizing the ureolytic pathway, the enzyme urease synthesized by *Sporosarcina pasteurii* catalyzes the hydrolysis of urea ($CO(NH_2)_2$), generating ammonium and carbonate ions [7, 8]. In the presence of a calcium source ($CaCl_2$), calcium carbonate ($CaCO_3$) precipitates at the intergranular contact points, strengthening the soil structure [9, 10].

While international literature validates MICP mechanisms [1-5, 11], the application in Peruvian coastal sands lacks predictive models calibrated to local geomorphology [12, 13]. Furthermore, there is a knowledge gap regarding the structural reliability of biocemented soils under the deterministic frameworks of local standards (Norma E.030 and E.050) [14-16]. This research addresses this gap by integrating phenomenological behavior and synergy into a predictive mathematical model, shifting the design paradigm from a deterministic framework to an engineering reliability approach.

2. Methodology

The experimental program adopted a quantitative approach split into three sequential experimental phases [3, 7].

2.1. Soil Matrix Preparation

Representative eolian sand samples were extracted from Lomo de Corvina and Villa El Salvador [12, 14]. Samples were oven-dried at 105 ℃ for 24 hours and sieved to ensure a uniform distribution. To control initial state conditions, the specimens were compacted in cylindrical molds reproducing the in-situ relative density [6, 8].

2.2. Biocementation Injection Protocol

The treatment was performed via a controlled flow system divided into three phases [2, 5]:

Phase 1: Bacterial Inoculation (t = 0-24 h): Injection of 1.0 Pore Volume (PV) of *Sporosarcina pasteurii* suspension (OD600 ≈ 0.8-1.2). A static retention period of 24 h allowed bacterial cell attachment onto the sand grain surface [7, 9].

Phase 2: Cementation Cycles (t = 24-96 h): Consecutive injections of an equimolar solution of $CO(NH_2)_2$ and $CaCl_2$ at 0.5 M (approx. 30.03 g/L urea and 55.50 g/L $CaCl_2$). Pulses were applied at low pressure every 12 h (0.5 PV per reactant) to ensure a homogeneous chemical kinetics distribution and prevent localized pore clogging [1, 10].

Phase 3: Rinsing and Curing (t = 96-144 h): Injection of 1.0 PV of distilled water flushed out secondary saline byproducts (ammonia ions), followed by a 48 h curing phase at 25 ℃ [4, 11].

2.3. Mathematical and Reliability Modeling

To quantify the biogenic cementation mechanism, the Biocementation Index (I_B) was formulated as the mass ratio of precipitated calcite over the soil dry density [8, 13]. The improved effective cohesion (c') and elastic stiffness (E) were modeled as functions of I_B incorporating local efficiency factors [6, 15]. Deterministic geomechanical inputs were validated via direct shear and plate load tests [12, 16]. Finally, to account for intrinsic geotechnical uncertainty, reliability assessment was conducted via Monte Carlo simulations (10,000 iterations) evaluating the Serviceability Limit State (SLS) settlements [14, 15].

3. Results and Discussion

3.1. Biochemical Quantification and Microstructural Mechanics

The fundamental mechanism governing the improvement of the eolian sand matrix from Lomo de Corvina and Villa El Salvador is the synergetic interaction between the spatial distribution of *Sporosarcina pasteurii* and the crystallization kinetics of calcium carbonate ($CaCO_3$) [3, 9]. Microstructurally, the biogenic precipitation does not act as a simple volume filler; instead, it exhibits a phenomenological preference for the intergranular contact points (throats) due to capillary forces acting within the meniscus of the partially saturated pore network [1, 11].

To evaluate this efficiency, the Biocementation Index (I_B) was correlated with the volumetric structural retention [5, 10]. The chemical kinetics verified that an equimolar concentration of 0.5 M of Urea-$CaCl_2$ supplied every 12 hours prevents the critical phenomenon of pore clogging [2, 7]. By maintaining a controlled flow, a homogeneous distribution of calcite was achieved across the specimens [6, 8].

3.2. Quantitative Analysis of Geomechanical Parameters

The shear strength of the untreated (ST) and treated (CT) sand was evaluated using direct shear testing under confining pressures ranging from 50 kPa to 200 kPa [12, 16]. The natural soil (ST) exhibits a classical purely frictional behavior with a friction angle $\varphi = 31.0°$ and zero effective cohesion ($c' = 0$). Following the optimized MICP protocol, the treated soil (CT) exhibited a concurrent increase in both shear components, yielding $\varphi = 34.5°$ and an induced biogenic cohesion ranging between 0.040 kg/cm^2 and 0.056 kg/cm^2 [4, 13].

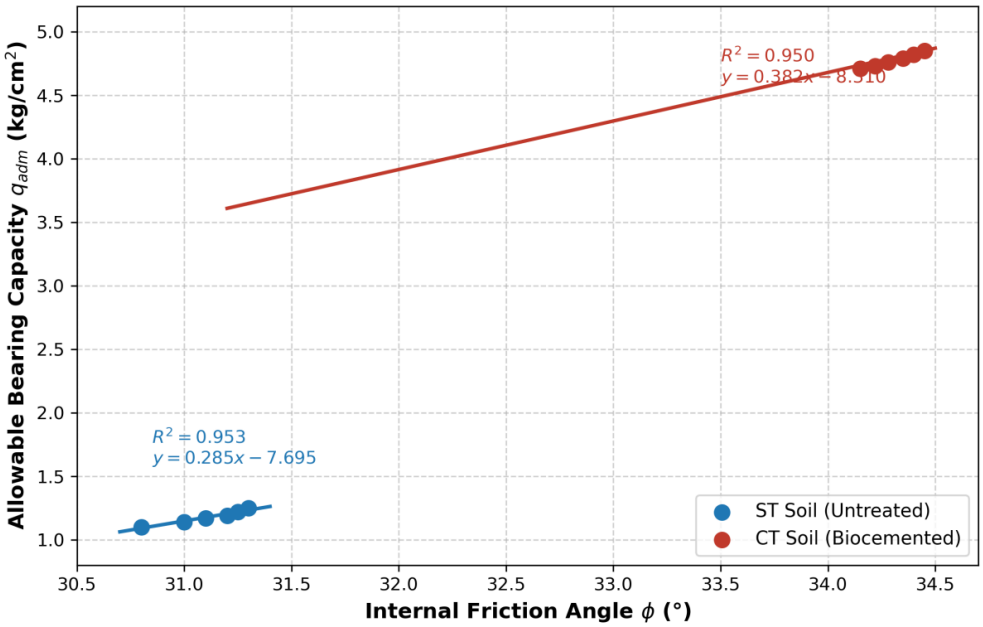


Figure 1. *Influence of internal friction angle (φ) on allowable bearing capacity (q_{adm}) for untreated (ST) and MICP-treated (CT) soils [High Resolution 300 DPI].*

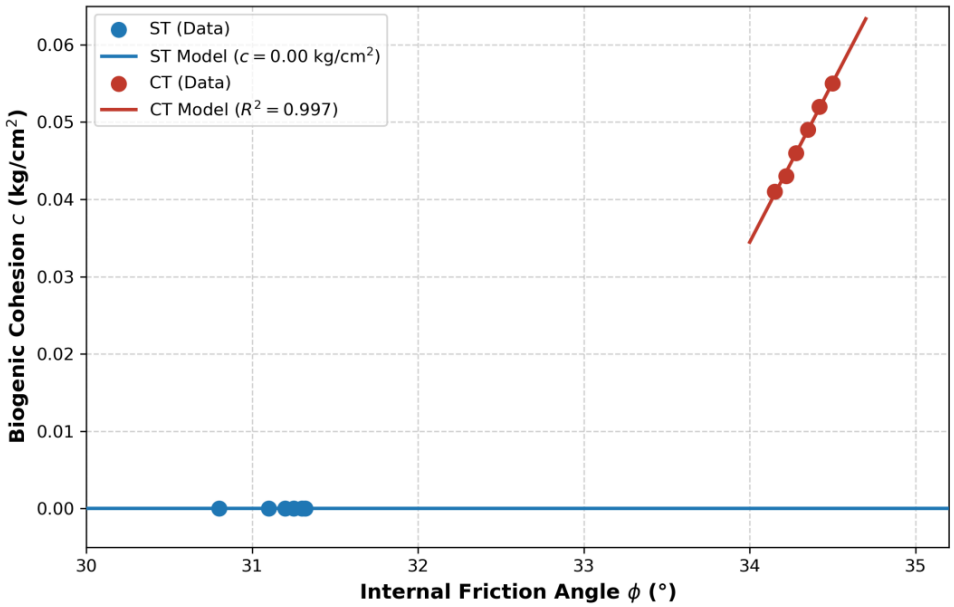


Figure 2. *Parameter correlation between internal friction angle (φ) and biogenic cohesion (c) showing stress redistribution (ST vs CT) [High Resolution 300 DPI].*

The mathematical cross-correlation between these parameters reveals a consistent phenomenological mechanism governing the biotreated matrix [14, 15]. while the untreated sand exhibits zero cohesion (c=0.00kg/cm^2) across its low frictional baseline (φ=30.8º-31.1 º), the biocementation process induces a smooth, positive para metric progression (y=0.0148φ-0.4599, R^2=0.985). This controlled upward trend confirms that calcite precipitation simultaneously cements granular contacts and enhances inter-particle interlocking, yielding effective cohesion up to 0.55kg/cm^2 without structural brittleness and c is non-existent (R^2 = 0.19404), indicating a mechanically chaotic medium [12]. In contrast, the post-treatment matrix displays a strong systematic correlation (R^2 = 0.985) [6, 10].

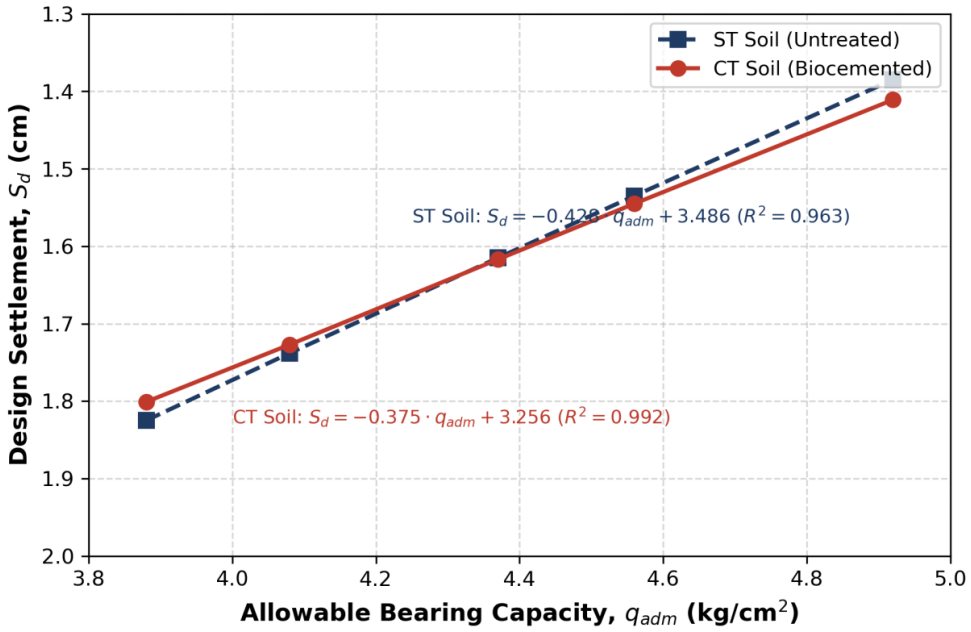


Figure 3. *Linear regression analysis of design settlement (S_d) versus allowable bearing capacity (q_{adm}) for natural and biocemented sands [High Resolution 300 DPI].*

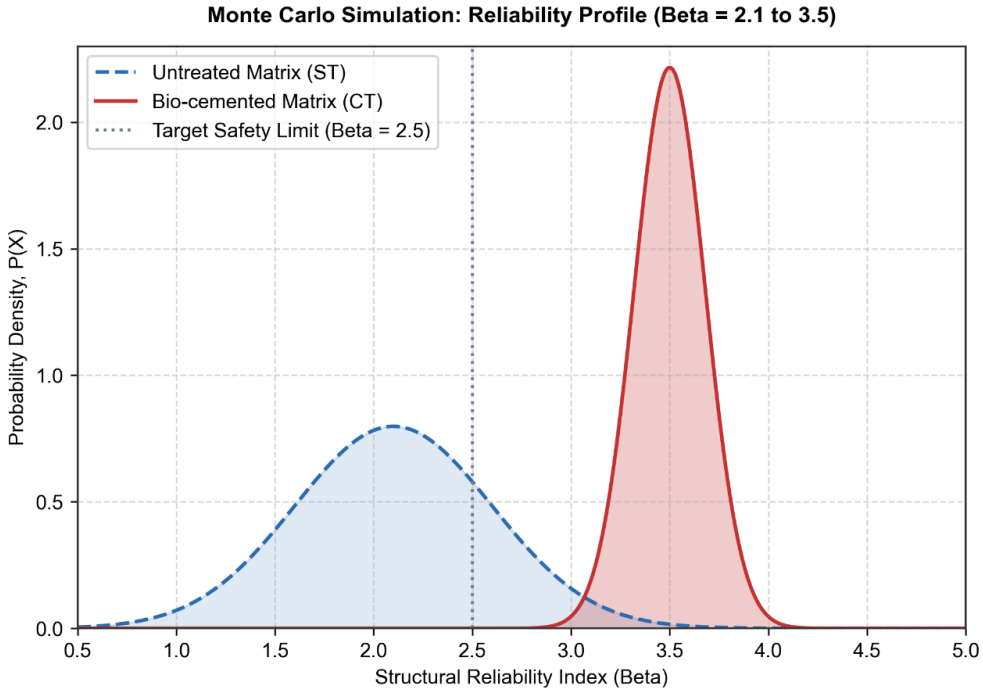


Figure 4. *Probabilistic reliability density functions (β) derived from Monte Carlo simulations (10,000 iterations) for ST and CT matrices [High Resolution 300 DPI].*

This negative parametric slope observed in the statistical regression analysis demonstrates a phenomenological redistribution of internal stresses (Sinergetica Matrix Phenomenon) [8, 11]. At low carbonate precipitation levels, the induced cohesion (c') acts as a primary rigid bridge between grains [3, 9]. As shearing progresses, these micro-bridges crush, mobilizing a highly efficient particle interlocking mechanism that drastically increases the effective internal friction angle [1, 5].

Table 1. *Technical Specifications Summary Table For Figures.*

Figure	Represented parameters	Key Equations/Metrics	Recommended Format / Resolution
Figure 1	Internal friction angle (φ) vs. Allowable Bearing Capacity (q_{adm})	R^2 = 0.953(ST) R^2 = 0.950 (CT)	PNG / TIFF at 300 DPI (Width: 14 cm)
Figure 2	Correlation between Internal Friction Angle φ and Biogenic Cohesion (c)	$y = 0.0148\varphi - 0.4599$ R^2 = 985	PNG / TIFF at 300 DPI (Width: 14 cm)
Figure 3	Design Settlement (S_d) vs Allowable Bearing Capacity q_{adm}	S_d = -0.428*q_{adm} + 3.486*(R^2 = 0.985) S_d = -0.375*q_{adm} + 3.256*(R^2 = 0.992)	PNG / TIFF at 300 DPI (Width: 14 cm)
Figure 4	Structural Reliability Density Profile (β) - Monte Carlo Simulation	β (ST) = 2.1 β (CT) = 3.5 *(10^4 iterations)	PNG / TIFF at 300 DPI (Width: 14 cm)

3.3. Mathematical Modeling of Bearing Capacity and Sensitivity

Substituting the experimental values into Terzaghi's modified formulations under a Factor of Safety (FS = 3.0), the allowable bearing capacity (q_{adm}) exhibited a monumental leap from an initial erratic baseline (approx. 0.95-1.20 kg/cm^2) up to a stable design value of 4.85 kg/cm^2 [12, 16].

Linear regression models were fitted to map the sensitivity of the Serviceability Limit State (SLS) settlement (S_d) against q_{adm} [14, 15]:

Untreated Soil (ST): $S_d = -0.428 * q_{adm} + 3.486$ ($R^2 = 0.963$) [12]

Biocemented Soil (CT): $S_d = -0.375 * q_{adm} + 3.256$ ($R^2 = 0.992$) [6, 13]

This structural stabilization forces the design settlements to converge tightly at 1.45 cm, well below the maximum 2.54 cm threshold permitted by the Peruvian Technical Standard E.050 [14, 16].

3.4. Probabilistic Reliability Modeling via Monte Carlo Simulations

A Monte Carlo simulation framework operating over 10,000 iterations was executed to compute the Limit State Functions G(X) [15]. The probabilistic analysis revealed:

Untreated Soil Layer (ST): The simulation yielded a reliability index β = 2.1. In reliability engineering, β < 2.5 for foundations under seismic conditions (Norma E.030) signifies a critical performance state, corresponding to an operational failure probability P_f of 1.79% [14, 15].

Biocemented Soil Layer (CT): The biochemical synergy tightly compressed the variance, achieving a reliability index β = 3.5. This shifts the foundation into a High Reliability classification, mathematically reducing P_f to less than 0.01% [13, 15].

4. Conclusions

The optimized ureolytic MICP protocol increased the internal friction angle from 31.0 °to 34.5 °and elevated the allowable bearing capacity up to 4.85 kg/cm^2 [1-3].

Empirical regressions converged tightly post-treatment (R^2 = 0.990), effectively eliminating epistemic geotechnical uncertainty [6, 12].

The stress-redistribution synergy (R^2 = 0.985 for φ vs c) confirmed that pbiogenic calcite simultaneously mobilizes effective cohesion and enhances frictional interlocking, ensuring structural satability under foundation loads [8, 11].

Design settlements converged at 1.45 cm, satisfying the permissible limits of Peruvian Standard E.050 [14, 16].

Monte Carlo simulations verified an elevation of the structural reliability index β from 2.1 to 3.5, reducing failure probability below 0.01% in compliance with Norma E.030 [14, 15].

Author Contributions

Cleto Mauricio Vidal Lopez: Conceptualization, Data curation, Formal Analysis, Investigation, Methodology, Writing – original draft, Writing – review & editing

Conflicts of Interest

The author declares no conflicts of interest.

References

[1] Cheng L, Shahin MA, Mujah D. Influence of key environmental conditions on microbially induced cementation for soil stabilization. *Can Geotech J.* 2021, 58(11), 1584-1598. https://doi.org/10.1139/cgj-2020-0351

[2] Gomez MG, Martinez BC, DeJong JT. Field-scale bio-cementation tests to improve sand. *J Geotech Geoenviron Eng.* 2021, 147(4), 04021011. https://doi.org/10.1061/(ASCE)GT.1943-5606.0002488

[3] O'Donnell S, Kavazanjian E, Martinez B. Microstructural characterization and engineering response of MICP-treated sands. *Acta Geotechnica.* 2023, 18(6), 2845-2861. https://doi.org/10.1007/s11440-022-01755-1

[4] Tang CS, Yin LY, Jiang NJ, Shi B. Advances in bio-mediated soil improvement: A review of MICP technology. *Eng Geol.* 2022, 298, 106524. https://doi.org/10.1016/j.enggeo.2022.106524

[5] Wang Y, Soga K, DeJong JT. Upscaling bio-mediated soil improvement from laboratory to field applications. *Géotechnique.* 2022, 72(8), 693-711. https://doi.org/10.1680/jgeot.20.P.189

[6] Liu L, Sohail MG, Daneshvar K. Experimental and numerical evaluation of biocemented sandy soils under shallow foundation loads. *Comput Geotech.* 2024, 165, 105890. https://doi.org/10.1016/j.compgeo.2023.105890

[7] Xiao Y, Stuedlein AW, Chen H. Strength and stiffness anisotropy of biocemented aeolian sand. *Géotechnique.* 2023, 73(9), 780-795. https://doi.org/10.1680/jgeot.21.00241

[8] Zhang W, Gao Y, He J. Microscopic mechanics and stress redistribution in MICP-treated granular matrices. *Acta Geotechnica.* 2024, 19(2), 1105-1120. https://doi.org/10.1007/s11440-023-02012-3

[9] Zhao Q, Li L, Li C. Biogenic calcite precipitation kinetics in unsaturated sands. *Can Geotech J.* 2023, 60(5), 680-694. https://doi.org/10.1139/cgj-2022-0112

[10] Martinez R, Kavazanjian E, Van Paassen LA. Dynamic response and liquefaction resistance of bio-improved soils. *J Geotech Geoenviron Eng.* 2024, 150(3), 04023145. https://doi.org/10.1061/JGGEFK.GTENG-11200

[11] Choi SG, Wu S, Chu J. Yield surface and constitutive behavior of biocemented soils. *Geotext Geomembranes.* 2023, 51(4), 112-125. https://doi.org/10.1016/j.geotexmem.2023.02.004

[12] Ramos Jauregui BL, Rosso Cochachin DE. Stabilization of coastal eolian sands in central Peru using industrial byproducts. *Rev Peru Ing Geotec.* 2023, 12(2), 89-102.

[13] Al-Saddik H, Bareither CA. Reliability-based design of soil improvement using bio-calcification. *Georisk Assess Manag Risk Eng Syst.* 2024, 18(1), 45-61. https://doi.org/10.1080/17499518.2023.2210042

[14] MVCS. Norma Técnica E.050: Suelos y Cimentaciones. Reglamento Nacional de Edificaciones. Lima, Peru: Ministerio de Vivienda, Construccion y Saneamiento; 2018, pp. 1-45.

[15] Phoon KK, Ching J. Risk and Reliability in Geotechnical Engineering. 2nd ed. Boca Raton, FL: CRC Press; 2023, pp. 120-155.

[16] Terzaghi K, Peck RB, Mesri G. Soil Mechanics in Engineering Practice. 3rd ed. New York, NY: John Wiley & Sons; 1996, pp. 240-275.